Proceeding of the 2015 IEEE
International Conference on Information and Automation
Lijiang, China, August 2015

Multi-UAVs Formation Control Based on Artificial Physics

Huan Liu, Xiangke Wang and Huayong Zhu
College of Mechatronic Engineering and Automation,
National University of Defense Technology, Changsha 410073, China
xkwang@nudt.edu.cn

***Abstract* - In this paper, we propose a control method based on the artificial physics and leader-follower strategy for the multiple Unmanned Aerial Vehicles (UAVs) formation control. Compared with the existing methods, the main contribution of this paper is that we design a formation controller based on the modified artificial physics for the fixed-wing UAVs with the velocity and roll angle constraints and the real quadrotor systems. The advantages of our control strategy are simple, scalable, robust and distributed.**

Index Terms - UAV formation, artificial physics, autopilot.

I. INTRODUCTION

The UAVs formation control has aroused many researchers' interests. In recent decades, different methods have been proposed to solve the formation control problems, such as the leader-follower strategy, the virtual structure strategy, the behavior-based strategy, the artificial field strategy and the graph-based strategy[1]. In this paper, we propose a new control strategy based on the artificial physics. The artificial physics is first proposed by William M. Spears[2]. At first, the artificial physics method is used to self-organize swarms of mobile robots into hexagonal formations. Inspired by the law of universal gravitation, William M. Spears creates the forces between two agents. Through the attractive and repulsive forces between two agents, the swarms can make the convergence behavior and avoidance behavior[3][4]. Though the artificial physics method has some advantages such as self-assembly, fault-tolerance , self-repairs, briefness and distribution, it also has some shortcomings such as easily plunging into a local optimal solution, longer settling time and rough trajectories[5]. What's more, the traditional artificial physics method can only form the hexagonal lattices, not the formation desired. The traditional artificial physics is designed for the omnidirectional agents, and not suitable for the nonholonomic systems such as the fixed-wing UAVs. In order to overcome some shortcomings of the traditional artificial physics, we design a new controller for the omnidirectional UAVs like quadrotors and the fixed-wing UAVs respectively. The controllers that we design can also realize the desired standard formation which is the basic formation for transforming into another arbitrary formation.

The rest of the paper is organized as follows. In Section II, we construct the standard formation model. The formation control design based on the modified artificial physics method for the quadrotors and fixed-wing UAVs is proposed in Section III.

II. THE STANDARD FORMATION MODEL

We define the standard formation as a regular polygon with n sides. The UAVs lie on the circumcircle evenly, and the length of each side is equal to L. The circumcenter of the polygon is in a desired position x_c. R is the radius of the circumcircle of the polygon. Fig.1 shows the standard formation.

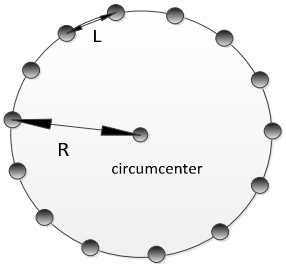

Fig.1 The standard formation

Our aim is to design a controller to drive the UAVs to form the standard formation.

This formation model is different from the traditional artificial physics model. In the traditional artificial physics model[6], the agent is regarded as a mass point. Every agent is drove by the artificial force:

$$F = Gm_i m_j / r^p , \quad (1)$$

where F is the magnitude of the force between two particles i and j, and r is the range between the two particles. P is some power(usually $p = 2$). G is set at initialization. The force is repulsive if $r \le R$ and attractive if $r > R$. Thus each agent can be considered to have a circular "potential well" around itself. Under this force law, seven agents will force a regular hexagon
with a agent at the center as Fig.2 shows. As the number of the agents increasing, the agents will form a hexagonal lattice as Fig.3 shows.

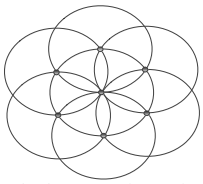
Fig.2 The hexagon formation

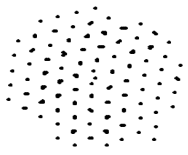
Fig.3 The hexagonal lattice

Actually, by artificial physics force law, the agents can't form the desired formation like the standard formation shown

in Fig.1 as the number of agents increasing. So we should modify the artificial physics law.

III. The Modified Artificial Physics Law

A. Formation Control for the Model of Point Mass UAV

In the rest of the paper, we use five agents as the example to build the modified artificial physics law and do the simulations. The standard formation topology with five UAVs is as Fig.4 shows:

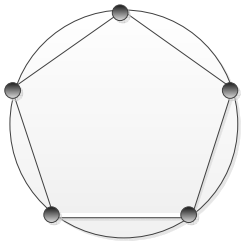

Fig.4 The standard formation topology with five UAVs

Firstly, we should define the force law. The mass of the every UAV is 1 by default. The attractive force is as follows:

$$f_{ija} = \begin{cases} G(\|r_{ij}\| - L) r_{ij} / \|r_{ij}\|, \|r_{ij}\| > L \\ 0, \|r_{ij}\| \le L \end{cases}, \quad (2)$$

where f_{ij} is the force between the i_{th} UAV and the j_{th} UAV. $r_{ij} = X_j - X_i$ is the relative position vector. X_j and X_i are the positions of the i_{th} UAV and the j_{th} UAV respectively. As we can see, if the $\|r_{ij}\| > L$, it will produce the attractive force to drive the i_{th} UAV toward the j_{th} UAV. But when the distance between two UAVs is smaller than *L*, the attractive force will vanish, and the repulsive force will work. We define the repulsive force as follows:

$$f_{ijr} = \begin{cases} G(\|r_{ij}\| - L) r_{ij} / \|r_{ij}\|, \|r_{ij}\| \le L \\ 0, \|r_{ij}\| > L \end{cases}. \quad (3)$$

We can combine (3) with (4) to one force law:

$$f_{ij} = G(\|r_{ij}\| - L)\vec{r}_{ij} / \|r_{ij}\|. \quad (4)$$

Assume that every UAV has a sensor range S_R. When other UAV approaches with a distance smaller than $L(L< S_R)$, then the repulsive force works.

It is worth to point out that the repulsive force is essential in the system in order to avoid collision. But the attractive force between two UAVs may not be essential because the more forces implied on the UAV, the more local minima points are resulted in.

At the circumcenter, there is a leader of the formation which is real or virtual. The other UAVs are regarded as followers. The control strategy is as follows:

1. The leader applies the attractive and repulsive force to every other UAV. Driven by the forces applied by the leader at the circumcenter, every other UAV can be located on the circumference.

2. There are repulsive forces between the UAVs avoiding collisions. Once the distance between two UAVs is less than L, there will be repulsive force between the two UAVs.

According to the above strategy, if we want to drive the agents to distribute on the circumcircle with x_c as the circumcenter, we should add another force:

$$f_c = G\frac{(\|r_{ic}\| - R) r_{ic}}{\|r_{ic}\|}. \quad (5)$$

where $r_{ic} = x_c - x_i$ is the relative position vector, and x_c and x_i represent the positions of the circumcenter and the i_{th} UAV respectively.

Combining the (3) with (4), we can obtain the sum forces implied on the followers:

$$f_i = \sum_{j=1, j\neq i}^{N} f_{ijr} + f_c \quad (6)$$

The force designed above can drive the UAVs to form the standard formation. In fact, there are infinite possible polygons lying on the same circumcircle because of the freedom of rotation. So we should add an extra force to eliminate that degree of freedom.

We find a point x^* on the circumcircle as an attractive point. If the distance between a follower and x^* is less than L^*, there will be attractive force between them until the follower occupy the position of x^*. Meanwhile, other UAVs will adjust their own positions to arrive at the new equilibrium point. We define the L^* as the attractive range. The value of the L^* is computed according to the fact that we must ensure that at any time ,only one UAV locates in the attractive range. We can compute the L^* according to the Fig.5.

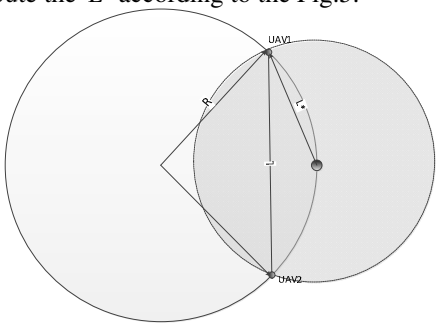

Fig.5 the value of L^*

We can obtain the value of the L^*:

$$L^* = L / \{2\cos[(\arcsin(L/2R))/2]\}.$$

The force between the UAV in the attractive range and the x^* is:

$$f_o = G * (\vec{x}_i - \vec{x}^*).$$

In order to eliminate oscillations, we add the damping term. So the sum forces applied on the followers are:

$$f_i = \sum_{j=1, j\neq i}^{N} f_{ijr} + f_c + f_o - b\dot{x}_i \quad (7)$$

Proposition 1: The UAVs modelled as the point mass will form the standard formation driven by the force law (7), and the configuration is asymptotically stable.

Proof:

In this paper , we model the i_{th} UAV as follows:

$$\ddot{x}_i = u_i,$$
$$u_i = \sum_{j=1, j\neq i}^{N} f_{ijr} + f_c + f_o - b\dot{x}_i. \tag{8}$$

Let $\tilde{x} = [x_1^T, \cdots, x_N^T, \dot{x}_1^T \cdots, \dot{x}_N^T]^T$ be the state vector of the system.

We construct a lyapunov function:

$$V(\tilde{x}) = \sum_{i=1}^{N}\left[V_{ic} + V_{iar} + V_{io} + \frac{1}{2}\|\dot{x}_i\|^2 \right] \tag{9}$$

where

$$V_{ic} = \frac{1}{2}G*(\|r_{ic}\| - R)^2 \tag{10}$$

$$V_{iar} = \frac{1}{2}G*(\sum_{j=1, j\neq i}^{N}(\|r_{ij}\| - L)^2) \tag{11}$$

$$V_{io} = \frac{1}{2}G*\|x_i - x^*\|^2 \tag{12}$$

Obviously, $V(\tilde{x}) \geq 0$,and $V(\tilde{x}) = 0$ if and only if $\|r_{ic}\| = R$, $\|r_{ij}\| \geq L$, $\|x_i - x^*\|$,and $\|\dot{x}_i\|$=0.

Consider the time derivative of the function (9), we have that:

$$\dot{V}(\tilde{x}) = \sum_{i=1}^{N}\dot{x}_i^T[\frac{\partial V_{ic}}{\partial x_i} + \frac{\partial V_{iar}}{\partial x_i} + \frac{\partial V_{io}}{\partial x_i} + \ddot{x}_i] \ , \tag{13}$$

$$\begin{aligned}\ddot{x}_i &= \sum_{j=1, j\neq i}^{N} f_{ijr} + f_c + f_o - b\dot{x}_i \\ &= \frac{\partial V_{iar}}{\partial x_i} + \frac{\partial V_{ic}}{\partial x_i} + \frac{\partial V_{io}}{\partial x_i} - b\dot{x}_i\end{aligned}. \tag{14}$$

So,

$$\dot{V}(\tilde{x}) = -b\sum_{i=1}^{N}\|\dot{x}_i\|^2 \leq 0.$$

According to the LaSalle's principle, the desired configuration is asymptotically stable.

B. Formation Control for the Quadrotors

The control strategy above aim at the point mass model. Because the quadrotor is a omnidirectional system, it can be modelled as a point mass. Actually, (7) indicate the desired velocity vector. Through the control strategy (7) above, we can get the desired velocity v_{dx} , v_{dy} in x-axis and y-axis respectively and the desired heading angle ψ_d. We assume that the UAVs are at the same altitude, so the desired velocity in z-axis v_{dz} is zero. For the real control system of the quadrotor, we must map the desired velocity to the control system of the quadrotor. So we adopt the ADRC control strategy. The dynamic model and more detail can be referred in [7]. The control structure is as Fig.6 shows, where θ_d and ϕ_d are the desired pitch angle and roll angle, and $\Omega_1 - \Omega_4$ are the four rotors speeds respectively.

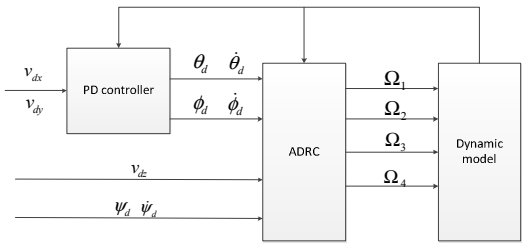

Fig.6 The ADRC control structure for the quadrotor

Fig.7 shows the convergence trajectories of five omnidirectional quadrotors. Fig.8 shows the positions of the five quadrotors at the end of convergence process.

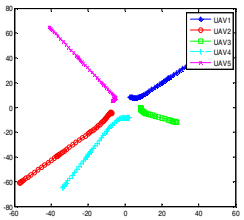

Fig.7 The convergence trajectories of five omnidirectional UAVs

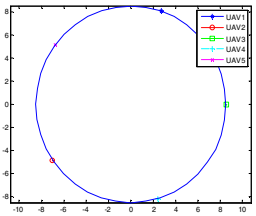

Fig.8 The positions of the five UAVs at the end of convergence process

From Fig.7-8, we can see that the force law (7) can drive the quadrotors to form the standard formation.

The control law above is suitable for the omnidirectional UAV not for the fixed-wing UAV. Because the fixed-wing UAV is a nonholonomic system, and it can't do the lateral movement or back movement instantaneously. In addition, the fixed-wing UAV has velocity and roll angle constraints. So we should reconstruct the control law for the fixed-wing UAVs.

C. Formation Control for the Fixed-wing UAV

The UAV autopilot model with the velocity and roll angle constraints is[8]:

$$\begin{aligned}&\dot{x} = v\cos\psi, \dot{y} = v\sin\psi, \dot{\psi} = g\frac{\tan\phi}{v}, \\ &\dot{v} = \frac{1}{\alpha_v}(v_c - v), \dot{\phi} = \frac{1}{\alpha_\phi}(\phi_c - \phi), \\ &\ddot{h} = -\frac{1}{\alpha_{\dot{h}}}\dot{h} + \frac{1}{\alpha_h}(h_c - h), \\ &0 < v_{\min} \leq v \leq v_{\max}, \\ &-\phi_{\max} \leq \phi \leq \phi_{\max},\end{aligned} \tag{15}$$

where $\alpha_v, \alpha_\phi, \alpha_h$ are the system constant. In this paper, we neglect the control of altitude, assuming that all the UAVs are at the same altitude.

From section *A*, we can obtain that:

$$\begin{aligned} \ddot{x}_i &= u_i \\ u_i &= \vec{F}_i / m \end{aligned}, \tag{16}$$

$$\vec{F}_i = \sum_{j=1, j\neq i}^{N} f_{ijr} + f_c + f_o - b\dot{x}_i, \tag{17}$$

where m is 1 by default. From (16), we can obtain the expected velocity value and the expected heading angle of the UAV i denoted as $v_{id}(t)$ and $\psi_{id}(t)$ at time t:

$$\begin{aligned} \vec{F}_i &= \sum_{j=1, j\neq i}^{N} f_{ijr} + f_c + f_o - b\dot{x}_i \\ u_i &= \vec{F}_i \\ \vec{v}_{id} &= \int u_i \\ v_{id} &= \|\vec{v}_{id}\| \end{aligned}, \tag{18}$$

$$\psi_{id} = \begin{cases} -\pi/2, v_{idx} = 0, v_{idy} \le 0, \\ \pi/2, v_{idx} = 0, v_{idy} \ge 0, \\ -\pi + \text{atan}(v_{idy}/v_{idx}), v_{idx} < 0, v_{idy} < 0, \\ \pi + \text{atan}(v_{idy}/v_{idx}), v_{idx} < 0, v_{idy} > 0, \\ \text{atan}(v_{idy}/v_{idx}), else \end{cases}$$

where v_{idx} and v_{idy} are the components of the v_{id} in *x-axis* and *y-axis*.

If we input the expected velocity value to the autopilot, we can obtain that:

$$\dot{v}_i = \frac{1}{\alpha_v}(v_{id} - v_i) \tag{19}$$

We can't input the expected heading angle to the autopilot directly, because the input variable in the autopilot is the roll angle. So we should obtain the expected roll angle by the heading angle. The relationship between the roll angle and the heading angle is as follows:

$$\dot{\psi}_i = g\frac{\tan\phi_i}{v_i} . \tag{20}$$

So the expected roll angle ϕ_d is:

$$\phi_{id} = \arctan(k(\psi_{id} - \psi_i)v_i / g) . \tag{21}$$

From (18)-(21), We can obtain the whole control strategy:

$$\dot{v}_i = \frac{1}{\alpha_v}(v_{id} - v_i), \dot{\phi}_i = \frac{1}{\alpha_\phi}(\phi_{id} - \phi_i) . \tag{22}$$

We have prove the stability of the point mass model in section *A*. For model (15), we just map the expected velocity value and the expected heading angle obtained from the section *A* to the autopilot of the fixed-wing UAV. So we just prove that the autopilot can make the real velocity and roll angle tend to the expected velocity value and the expected heading angle. Obviously, the autopilot can make it as (22) shows.

By the control strategy (22), the positions of the five UAVs at some time while maneuvering as Fig.9 shows. We can see that the five UAVs keep the standard formation while maneuvering. Fig.10 shows the trajectories of five UAVs while maneuvering. Fig.11 and Fig.12 show the velocities and roll angles of the five UAVs.

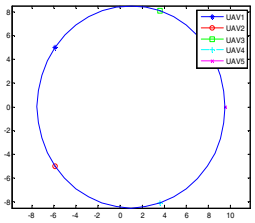

Fig.9 The positions of the five UAVs at some time while maneuvering

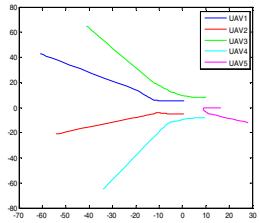

Fig.10 The trajectories of five UAVs while

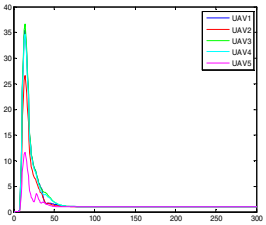

Fig.11 the velocities of the five UAVs respectively

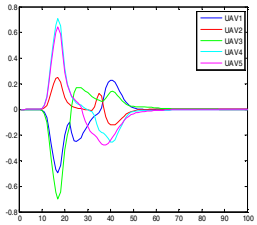

Fig.12 the roll angle of the five UAVs respectively

From Fig.11 we can see that all the values of the five UAVs' velocities is less than 40. If the velocity constraint is $1 \le v \le 30$, obviously the velocities of UAV 3 and UAV 4 don't meet the velocity constraint. So we should add an extra constraint to the controller (22):

$$v_{id} = 30 \text{ ,if } v_{id} \ge 30.$$

Fig.12 shows the roll angles of the five UAVs while maneuvering. From Fig.12 we can see that $-0.8 \le \phi_{id} \le 0.8$, which usually meets the roll angle constraints. If the roll angle constraint is $-0.4 \le \phi \le 0.4$, we should add an extra constraints to the controller (22):

$$-0.4 \le \phi_{id} \le 0.4 \text{ , if } \phi_{id} \ge 0.4 \text{ or } \phi_{id} \le -0.4 .$$

If we add the velocity and roll angle constraints to the controller, the simulation result is as Fig.13-17 shows:

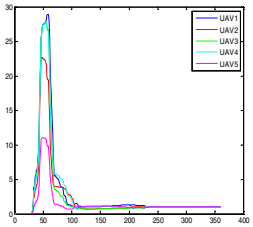

Fig.13 The velocities of five UAVs with velocity and roll angle constraints

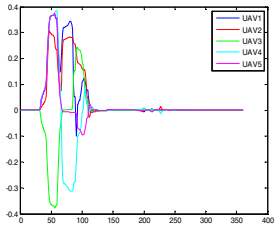

Fig.14 the roll angles of the five UAVs with velocity and roll angle constraints

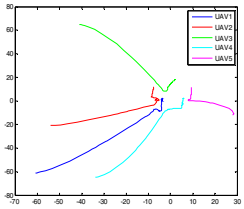

Fig.15 the trajectories of five UAVs while maneuvering with velocity and roll angle constraints

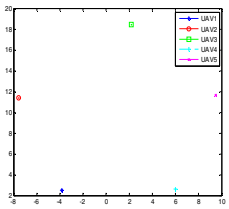

Fig.16 the positions of the five UAVs at some time while maneuvering with velocity and roll angle

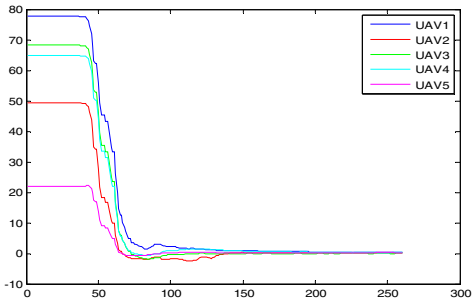

Fig.17 the distances between the five UAVs and the circumcenter

Comparing Fig.13-14 with Fig.11-12, we can see that after adding the velocity and roll angle constraint, the velocities and the roll angles are all in the range of constraint, but the settling time are longer. Eventually, the five UAVs can form the standard formation as Fig.16 shows. In order to validate our controller's applicability, We change the trajectories of the leader, so the trajectories shown in Fig.15 is different from Fig.12. Fig.17 shows the distances between the five UAVs and the circumcenter, from which we can see that all the distances approach zero.

IV. Conclusions

In this paper, we design controllers for the quadrotors and fixed-wing UAVs respectively based on the modified artificial physics. Driven by the controllers designed, UAVs can form the standard formation which overcoming the shortcoming of traditional artificial physics method that only seven agents can form the standard formation. The standard formation is very important. Actually, using the affine transformation, we can transform the standard formation into arbitrary formation which the traditional artificial physics cannot archive. For the fixed-wing UAVs formation controller, there is a shortcoming that after adding the velocity and roll angle constraints to the fixed-wing UAVs formation control, the system settling time is longer. So, in future work, we should redesign the controller to shorten the settling time and make the trajectories smoother.

References

[1] Guoqiang.W, "A Survey on Coordinated UAV Formation Management," *Electronics Optics and Control*,vol.20,no.8,2013.

[2] Spears W M, Gordon D F, "Using artificial physics to control agents," *In: Proceedings of the IEEE Conference on Information, Intelligence, and System. Bethesda MD: IEEE*, pp.281–288,1999.

[3] W.Spears, D.Spears, J.Hamann, and R.Heil, "Distributed, physics-based control of swarms of vehicles," *Autonomous Robots*,vol.17,no.2-3,2004.

[4] Spears W M, Spears D F, Heil R, et al, "An overview of physicomi-Metics," *Lecture Notes in Computer Science.* Berlin: Springer-Verlag Press, pp. 84–97,2005.

[5] Luo Q N, "An improved artificial physics approach to multiple UAVs/UGVs heterogeneous coordination," *Science China Technological Sciences*, vol.56, no.10,pp.2473-2479,2013.

[6] Spears W M, "Artificial physics for mobile robot formations," *System, Man and Cybernetics*, pp.2287-2292,2005.

[7] Wang Junsheng, Ma Hongxu, "Research on micro quadrotor control based on ADRC," *Journal of Projectiles , Rockets , Missiles and Guidance*, vol.28, no.3, 2008.

[8] Wei Ren, "Trajectory tracking control for a miniature fixed-wing unmanned air vehicle," *International Journal of Systems Science*, vol. 38, no. 4, pp.361–368,2007.